2016 IEEE Intelligent Vehicles Symposium (IV)
Gothenburg, Sweden, June 19-22, 2016

High-Precision Motion Control Method and Practice for Autonomous Driving in Complex Off-Road Environments*

Zhenping Sun, Zhenhua Huang, Qi Zhu, Xiaohui Li, and Daxue Liu

Abstract— **In the last decade, autonomous driving technology has become an important research topic due to its potential economic and social benefits. There has been considerable research activities contributed to make the autonomous driving system adapt to complex environments. Motion control is vital to the overall autonomous driving system, especially when the autonomous vehicle is driving in complex off-road environments. The aim of our work in this paper is to develop a high-precision motion controller for autonomous driving system running on rugged mountain roads and sand roads. Different from most existing methods in which the motion control problem is decoupled into lateral control and longitudinal control. In this work, a coupling controller is designed for solving the motion control problem of autonomous driving system. Experiments in the real-world rugged mountain road and sand road environment have been conducted to demonstrate the high-precision performance and efficiency of the proposed motion controller.**

I. INTRODUCTION

In recent years, autonomous driving technology has become an important research topic due to its potential economic and social benefits [1], [2]. There has been considerable research activities on making the autonomous driving system to adapt to more complex and challenging environments. In this paper an appropriate motion control method is developed for autonomous driving system in order to replace humankind to perform dangerous tasks, such as disaster-relief, tactical reconnaissance, etc.

The motion control problem is commonly defined as to control the vehicle's acceleration and steering, which makes it to track a predefined path given by the path planning module of an autonomous driving system. For a specific vehicle with a given motion mechanism, the control method may varies greatly. The research work of this paper only aims at car-like ground vehicles steered by front wheels and driven by internal combustion engine.

Path following is a general description of the autonomous driving system of our experimental vehicle. The path planning module generates a reference path and the length and the width of the planned path change according to the complexity of the road environment. The positioning system provides a measurement of the position, speed and orientation of the vehicle. The motion control module is to produce the control commands of steering, fuel and braking. Supposing that every control command is executed by the corresponding servo actuators accurately, the aim of our research is to design a motion control module for the autonomous driving system.

As a key problem of autonomous driving research, there has been substantial research in this area [3], [4], [5]. For the simplicity, the tracking control problem is often decoupled into two sub-problems: the lateral control and the longitudinal control. The lateral control only concerns about the lateral error between the vehicle and the reference path. On the other hand, the longitudinal control only concerns about the speed or position error of the vehicle to a desired signal. Actually this decoupling method is very effective under some ordinary conditions. In light of this idea, many control approaches have been proposed and tested [6], [7], [8], [9], [10].

For the lateral control problem, gain-scheduling and pure pursuit are two important methods. During the past years, many classic control methods have been used to solve this problem. In [11], a survey on many classic lateral controllers is introduced. In all of these methods, the reference path is described as a continuous curve. In addition, most of these methods need a parameter named preview distance, which is tuned according to the velocity of the vehicle. An exception is the method used by Stanley [12], [13], in which the preview distance is not needed. But a fairly smooth path is required in each replan circle. For the path planning module, the task of generating a smooth path at any time is difficult to fulfill. Besides, the high sensitivity to noise is another weak point of this method. A ribbon model based path tracking method is presented in [14]. The planned path is modeled as a ribbon in the proposed method, which takes the road width into account. In this way, it benefits the designing of the motion controller significantly. Based on the idea, the "preview distance" is also discarded permanently. Another benefit of employing this path model is to make the coupling between the lateral control and the longitudinal control become easier, which will be discussed in detail later.

For the longitudinal control problem, two major difficulties exist. One is the longitudinal dynamics modeling of the internal combustion engine driving vehicle. The other is the acceleration disturbance caused by mass variation, road slope, and the air resistance in different environments. Therefore, it is a troublesome task to design a specific speed following controller on every possible territory. The proportional-integral-derivative (PID) control [15] has a simple structure and is easy to implement as well. However, appropriate

*This work is supported by the National Natural Science Foundation-Joint Innovation and Development Foundation of Chinese Automobile Industry under Grant U1564214, National Natural Science Foundation under Grant 91220301.

Zhenping Sun, Zhenhua Huang, Qi Zhu, Xiaohui Li,and Daxue Liu are with College of Mechatronics and Automation, National University of Defense Technology, Changsha, 410073, P. R China sunzhenping_sx@139.com.

control parameters are difficult to be obtained when the control plant is a nonlinear system, such as the vehicle's longitudinal control system. As a robust control method, the sliding control is a proper candidate method for the vehicle's longitudinal control [16], [17]. A parametric longitudinal dynamic model is required in this method, whereas to build an accurate longitudinal model of the vehicle is a difficult task. An internal model controller based on a measured table model is designed in [18]. This method is much easier to manipulate, and the result of it is very attractive.

For the work of this paper, it is a continuance of our work in [14] and [18]. What we discuss about is to design a coupling controller for the motion control problem of autonomous driving in complex off-road environments.

The rest of our paper is organized as follows. Section II presents the whole structure of our designed motion controller. A variety of experimental results about the performance of motion control in the real-world rugged mountain road and sand road are illustrated in Section III. Finally, conclusions and some future work are discussed in Section IV.

II. BRIEF INTRODUCTION OF OUR COUPLING CONTROLLER

In this section, the controller structure of the motion control for our autonomous driving system is firstly presented. Then some controller modules designed for their special missions under the whole structure are introduced.

A. The Controller Structure of the Motion Control

Considering the complex of motion control problem, the effort of designing a single loop MIMO controller, which is expected to implement the mapping from given path to desired actuator commands, is doomed to be very difficult. Modularized multi-stage architecture is often used to simplify to the designing procedure [19]. This kind of architecture is also accepted in our autonomous driving system.

As illustrated in Figure 1, seven modules in our motion controller are presented, and three feedback loops are included. The *desired steering curvature computing* module is used to optimize the desired steering curvature based on the relationship between the vehicle and the planned path edge; the *acceleration/deceleration curve computing* module is used to set a desired velocity to every point of the desired path; *steering curvature controller* is used to improve the steer dynamic, compensate the disturbance, which makes the vehicle try to move with the desired curvature; the *acceleration/deceleration controller* is used to improve vehicle longitudinal dynamic feature, to compensate the disturbance from all kinds of factors; In the last layer, three servo modules are used to execute the control commands of steering, fueling, and braking. Among these seven modules, the three servo modules will not discuss in this paper detailed, for the reason that the servo-controllers using in our vehicle are the Whistle from ELMO, which is a mature ad hoc product. The seven modules loop constantly in each circle based on the feedbacks of the corresponding sensors mounted on the vehicle, which are illustrated in Figure 1. In the following, we will have a detailed discussion of the other four modules.

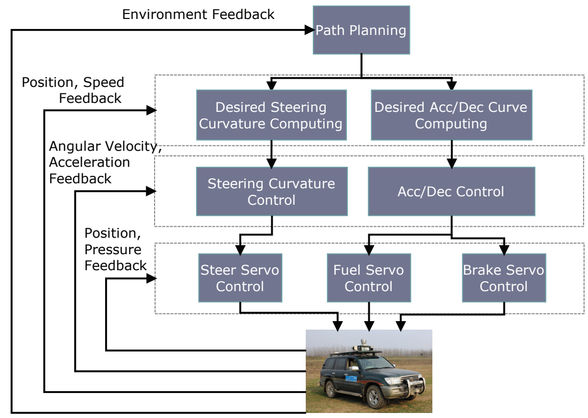

Fig. 1. The controller structure of the motion control.

B. Steering Curvature Controller

In this subsection, a steering curvature controller is designed to make the vehicle to track with the desired curvature obtained from its upper module. The steering dynamics of a car-like vehicle can be expressed as [14]:

$$\begin{aligned} mv(\dot{\beta}+\omega) &= -(k_f+k_r)\beta + \tfrac{l_r k_r - l_f k_f}{v}\omega + k_f\delta \\ &\quad + mg\sin(\alpha) + P_{ay}; \end{aligned} \tag{1}$$

$$I\dot{\omega} = (l_r k_r - l_f k_f)\beta - \frac{l_r^2 k_r + l_f^2 k_f}{v}\omega + l_f k_f \delta + P_{ay} l_{px}. \tag{2}$$

where:

- m — the mass of the vehicle, kg;
- I—the inertia of the vehicle, kg·m^2;
- v—the speed of the vehicle, m/s;
- ω —the yaw rate of the vehicle, rad/s;
- β —the sideslip angle of the mass center, rad;
- k_f, k_r —the stiffness of the front and rear wheel;
- δ —the steer angle, rad;
- l_f —the distance from the front wheel to the mass center, m;
- l_r—the distance from the rear wheel to the mass center, m;
- α —the lateral slope of the road;
- P_{ay}—the lateral aerodynamics;
- l_{px}—the distance between the aerodynamic center and the mass center, m.

For the steering curvature c, we have ω=vc. So the following equations can been derived:

$$\begin{aligned} mv(\dot{\beta}+vc) &= (l_r k_r - l_f k_f)c - (k_f+k_r)\beta \\ &\quad + k_f\delta + mg\sin(\alpha) + P_{ay}; \end{aligned} \tag{3}$$

$$I v \dot{c} = (l_r k_r - l_f k_f)\beta - (l_r^2 k_r + l_f^2 k_f)c + l_f k_f \delta + P_{ay} l_{px}. \quad (4)$$

Then the steer angle command δ can be computed via (3) and (4) if the steering curvature c is known. In real driving environment, parameters k_f, k_r in (3) and (4) are time varied. Therefore, to design a robust steering controller is a great challenge to an engineer. Some reasons may be concluded:

1) It is impossible to measure the lateral slope and aerodynamics in real-time, which should been taken as non-measurable disturbance;
2) Many parameters, such as k_f, k_l, l_f, l_r, m, change frequently, and cannot be measured directly;
3) The vehicle speed has a great influence on the steering dynamics.

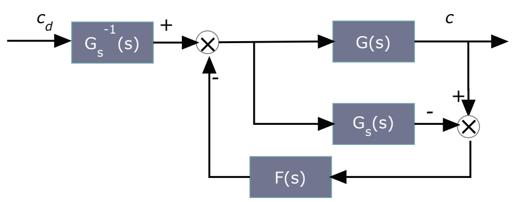

Fig. 2. The steering curvature controller based on an internal model.

After empirical tests, a steering curvature controller based on an internal model is designed to make the vehicle to track the desired curvature with high precision. In Figure 2, c_d is the desired curvature generated in the *desired steering curvature computing* module based on the path information and the vehicle's lateral error from the center of the desired path. More details about the procedures can be found in our previous work [14]. c is the measured current curvature of the current vehicle. δ denotes the exact steer angle to be sent to the *steering servo control module.* The controller fulfills the estimation task of the required steer angle δ based on the expected curvature and the vehicle's current dynamic information. $G(s)$ represents the actual steering system of vehicle. $G_s(s)$ denotes the nominal model of the steering system. For the simplicity of the inverse model, a steady state model of the steering system is used in our controller. $F(s)$ is a low-pass filter, which is designed to compensate the influence of the model error and the disturbance. Experiments below will illustrate the satisfied tracking performance of the proposed controller in complex off-road environments.

C. Desired Acceleration/Deceleration Curve Computing

As mentioned above, the steering dynamics are influenced greatly by the vehicle speed. The lateral error may be likely to increase as higher speed is reached. In order to control the lateral error of our path tracking system within a reasonable range, the desired speed output from the module of *Desired Acc/Dec Curve Computing* should be set properly. That means in some critical area such as the rugged mountain road and sand road, the coupling between lateral and longitudinal control is necessary for the vehicle to follow the desired path safely. This problem is the main topic and task of the *Desired Acc/Dec Curve Computing* module.

In Figure 3, $f(s)$ denotes the desired path given by the local path planning system. $f_l(s)$ and$f_r(s)$ are the left and right edges of the path, respectively. s denotes the station of the center line of the path. Based on empirical experiments and evaluations, six major factors which may influence the desired speed are derived: the length of the planned path, the distance of vehicle to road edges, path curvature, current path tracking error, steering error, and the acceleration/deceleration ability of the autonomous vehicle.

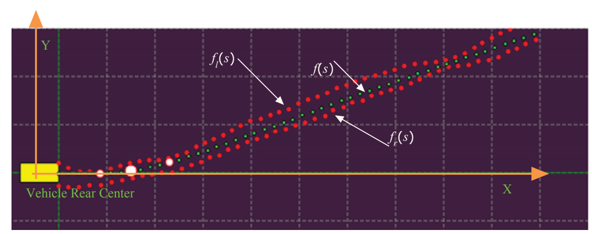

Fig. 3. The relationship between the vehicle and the planned path.

1) Length of the planned path
The length of path l_d is an important element which affects the desired speed. Actually at any time, the autonomous driving system has not enough knowledge about the road farer than l_d. Therefore, it is necessary and reasonable to assume that the vehicle could be stopped safely at end of current path in the emergency situation. So for any position i on the path the maximum desired speed can be expressed by:
$$v_{\max} = \sqrt{2 a_{\max} l_i} \quad (5)$$
where l_i is the distance of position i to the end of the path. $a_{\max}$ is the maximum deceleration that the vehicle can gain at the emergency situation.
2) Width of the planned path
The width of the planned path sets an error limit to the path tracking error. The tracking error should be no larger than half of the path width at any time. Otherwise, the safety of the autonomous vehicle would not be guaranteed. On the other hand, the lateral tracking error may increases with the increasing of vehicle speed. Therefore, the desired speed of the vehicle must be limited according to the width of the path. In this subsection, an empirical model is developed:
$$V_{max} < g(e) \quad (6)$$
where e refers to the desired error limit decided by the width of the path and the function of $g(\cdot)$ denotes a linear or polynomial function.
3) Path Curvature
In order to ensure the safety and comfort of our autonomous vehicle, the centrifugal force produced by

vehicle moving along a curved path should not be too large. Otherwise, a large sideslip will be generated and it may make the vehicle out of control, even rollover. The adhesion between the ground and the tires sets an upper limit to the maximum centrifugal force being allowed. In practice, considering the longitudinal acceleration of vehicle, the centrifugal force should be controlled under an even small limit. When considering the comfort of the passengers, the centrifugal acceleration should be smaller than $0.2g$. The relationship between the centrifugal acceleration and the vehicle speed is $a_c = v^2 c$, where a_c is the centrifugal acceleration, c is the path curvature. So it is very easy to get a speed limit according to path curvature:

$$v_{\max} = \sqrt{a_c/c} \tag{7}$$

4) Path Tracking Error
Experiments have demonstrated that a smaller tracking error can be achieved if the vehicle is slowed down. When the tracking error becomes too large, an initiative slowing down strategy can be used to reduce the tracking error within the desired range. As the same as the path width, there is also no analytic model, which can be derived to reflect the relationship between the path tracking error and the desired speed. In this paper, a reactive control strategy being used in our control module is suggested. If the lateral tracking error is out of the predefined range, the vehicle will be slowed down until the vehicle achieves the desired path.
5) Steering Servo Error
The steering angle command is sent to the *steering servo module*. The executive capacity of the command also has an impact on the tracking error. In the real control system, the steering servo error caused by the limitation of the steering actuator exists. When some dramatic changing path is encountered, the *steering servo module* needs to steer to the desired angle quickly. However, limited by the maximum power of itself, the steering actuator cannot satisfy this demand. Then a steering servo may appear, which means a large lateral error will be caused. If the phenomenon appears, the policy of slowing down the vehicle is actually the only choice can be adopted. We suggest an empirical function between the desired speed and steering servo error should be designed to limit the desired speed of vehicle.
6) The Acceleration/Deceleration Capability of the Vehicle
For a real autonomous vehicle, its acceleration/deceleration capability is finite. It is decided by the structure of the vehicle and the power of the engine. Any attempt to get an acceleration/deceleration out of the allowed limit is impossible. So the acceleration/deceleration ability must be considered when designing the speed curve.

Combining the six factors mentioned above, a feasible and reasonable speed curve along the desired path can be designed through the *desired acceleration/deceleration curve computing module*. Apparently, the speed curve is a result by coupling the lateral control with the longitudinal control during the autonomous driving. The procedure is really vital to the motion control in complex off-road environments.

D. Other Module of Our Controller

Two modules are remained to be discussed in our motion controller, which are the *desired steering curvature computing module* and the *acceleration/deceleration control module*. For this paper is a continuance of our work in [14] and [18], the methods in two papers are used in the two modules. More details about the *desired steering curvature computing module* and the *acceleration/deceleration control module* can be found in the two papers, if you are interested with them.

III. Experimental Results

In this section, experimental results of an autonomous land vehicle in rugged mountain road and sand road environments are exhibited to illustrate the effectiveness of our designed controller. The results are divided into three parts: (i) the desired speed planning on different types of the complex off-road environments with respect to (w.r.t) the *desired acceleration/deceleration curve computing module*; (ii) the speed tracking control w.r.t the *acceleration/deceleration control module*; (iii) the path tracking control w.r.t the *steering curvature computing module*.

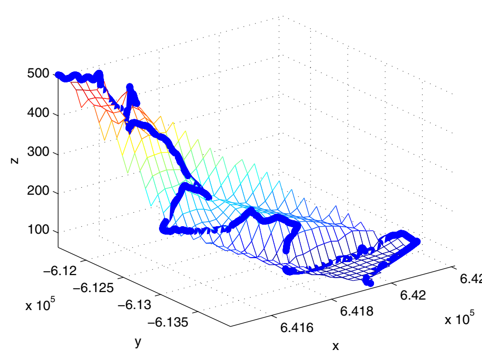

Fig. 4. A hill test route.

A. The desired speed planning

Figure 4 illustrates a hill test route during our experiment. Figure 5 shows four typical road conditions which our autonomous vehicle encountered during our experiment: (i) a wide and long road; (ii) a narrow road; (iii) an uphill road; (iv) a downhill road.

In the experiment, we demonstrate three main factors which have an effect on the planned speed: the length, the width and the curvature of the path. In Figure 6, different results of our local path planning are presented. If our vehicle is under road condition as shown in Figure 5(a), a long and wide path corresponding to Figure 6(a) is planned. If

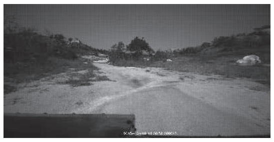

(a) A wide road

(b) A narrow road

(c) An uphill road

(d) A downhill road

Fig. 5. Typical encountered road conditions.

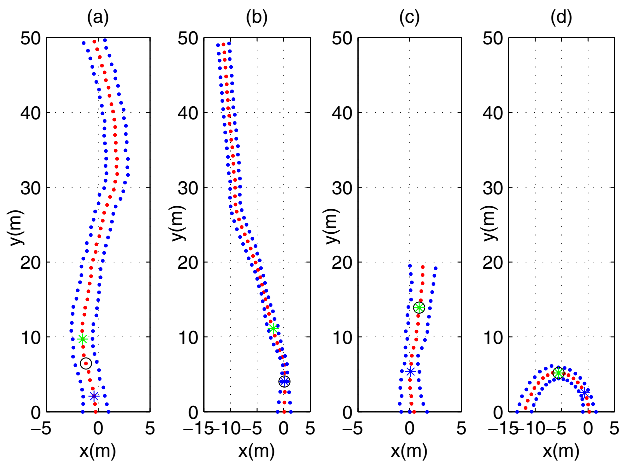

Fig. 6. Results of our local path planning.

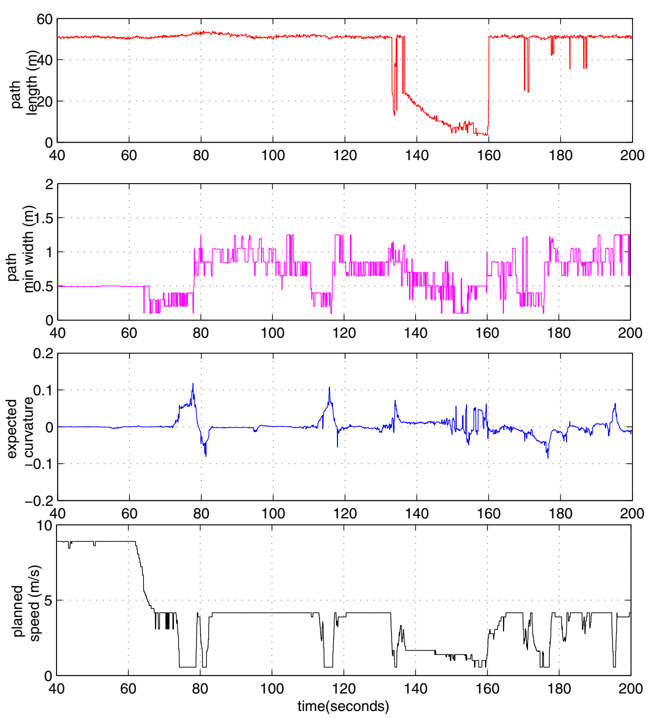

Fig. 7. The planned speed curve.

our vehicle is on a narrow road illustrated in Figure 5(b), a narrow path with respect to Figure 6(b) needs to be planned. When our vehicle is climbing a steep hill illustrated in Figure 5(c, d), the planned path may be short corresponding to Figure 6(c) for the sensing distance maybe decreased. If no road is available ahead of the vehicle, a U-turn action shown in Figure 6(d) may be required. It is reasonable to slow down the vehicle when a narrow path, a short path, or a path with turning is encountered.

Figure 7 shows the planned speed curve varying with the length, minimal width, and the expected curvature of the planned path. Our designed controller can slow down the vehicle effectively under different results of the local path planning to guarantee the tracking precision and safety of the autonomous vehicle.

B. Speed Tracking Control

In this part, the performance of our speed tracking controller is evaluated under two typical sand roads: (i) a sand road with pot-holes of different sizes ; (ii) a squared test field with sands and pot-holes on the ground. During the experiment, the steer is controlled by human.

(a) The sand road

(b) A sand squared test field

Fig. 8. The road for speed tracking control test.

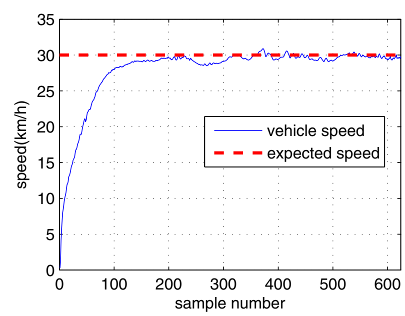

(a) The desired speed is 30km/h

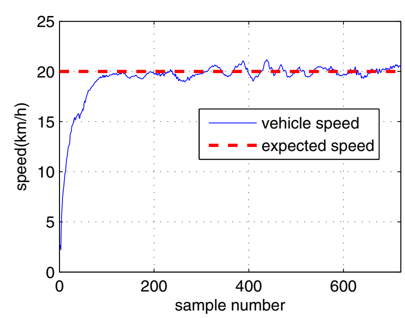

(b) The desired speed is 20km/h

Fig. 9. The speed tracking results on the sand road.

TABLE I
PERFORMANCE OF THE SPEED TRACKING CONTROL AFTER THE VEHICLE REACH THE TARGET SPEED STEADILY ON THE SAND ROAD.

$v_d(km/h)$	30	20
$max(\|\Delta v\|)(km/h)$	0.888	1.168
$var(\Delta v)$	0.125	0.198
$max(\|\Delta v\|)/v_d$	2.96%	5.84%

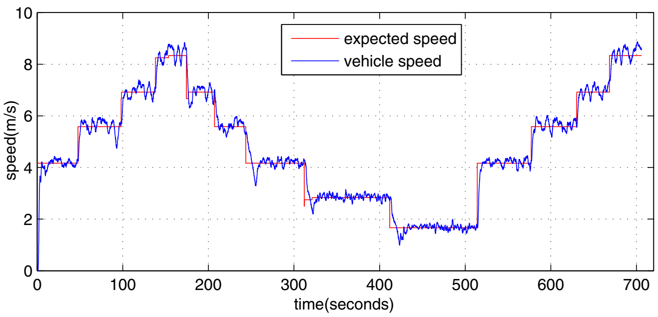

Fig. 10. The speed tracking results in a sand squared test field.

1) Sand road: Figure 8(a) shows the scene of the sand road. And Figure 9 illustrates the speed tracking results of the vehicle on the sand road when different desired speeds are set. Table I presents the performance of the speed tracking control after the vehicle reach the target speed steadily. v_d and Δv denotes the desired speed and the speed error, respectively. Though many holes exist on the sand road, the speed tracking error of our controller is keeping within a satisfied range.

2) A sand squared test field: A sand squared test field is shown in Figure 8(b). And Figure 10 illustrates the speed tracking results of the vehicle on the sand road when different desired speeds are set. Though the vehicle suffers with large disturbance caused by the sand road surface resistance, our designed controller is capable to track the set speed within the reasonable error bound.

C. Path Tracking Control

In this section, an experiment about path tracking control on a sand road is conducted to evaluate the performance of our designed steering curvature controller. Figure 11(a) shows the test route in the satellite imagery, and Figure 11(b) plots the tracking result in which the start point is set as the base point (0, 0). The details about the tracking results in the different parts are also demonstrated in Figure 12. The maximal path tracking errors of the four parts are about 0.1m, 0.2m, 0.5m and 0.6m, respectively. The experimental results show that the precision of the path tracking control on the sand road is satisfied.

IV. CONCLUSIONS

In this paper, a high-precision motion controller is proposed and the whole control structure of our autonomous

(a) The global path

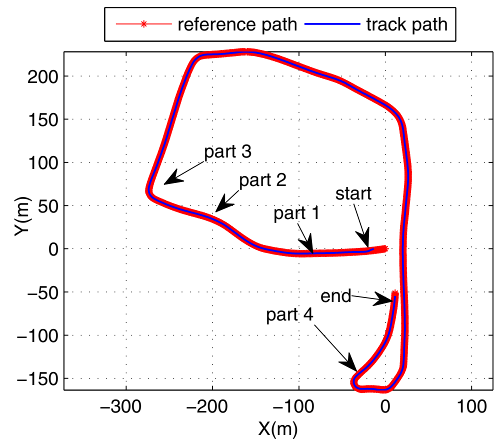

(b) The tracking result

Fig. 11. The test route in the satellite imagery and the whole path tracking results.

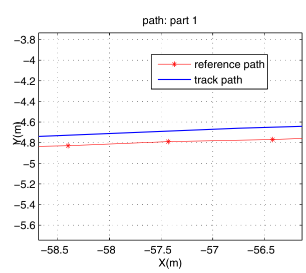

(a) Path tracking details of Part 1

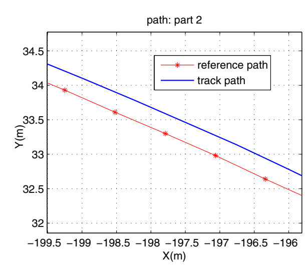

(b) Path tracking details of Part 2

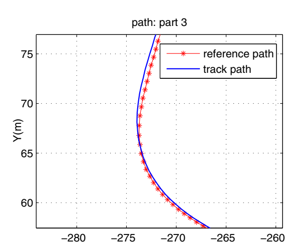

(c) Path tracking details of Part 3

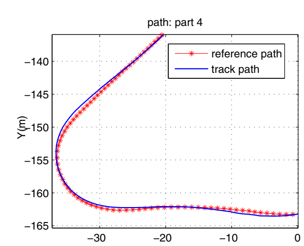

(d) Path tracking details of Part 4

Fig. 12. The details about the path tracking results in the different parts.

driving system is exhibited. Seven modules are mentioned in our motion controller:

- the *desired steering curvature computing* module;
- the *acceleration/deceleration curve computing* module;
- the *steering curvature controller*;
- the *acceleration/deceleration controller*;
- the *steering servo controller*;
- the *fuel servo controller*;
- the *brake servo controller*.

The tasks with respect to each controller are introduced, especially for the *steering curvature controller* and the *acceleration/deceleration curve computing* module. In the *acceleration/deceleration curve computing* module, six factors which affect the speed curve along the desired path are concluded. The speed curve is a result by coupling the lateral control with the longitudinal control during the autonomous driving. The procedure is really vital to the motion control in the complex off-road environments. Finally, experiments on the real-world rugged mountain roads and sand roads have been conducted to validate the high-precision and efficiency of our designed motion controller. Though some promising results have been obtained, much experience and time are still required during the experiments. Therefore, our future work may refer to some autonomous learning from the observed data.

ACKNOWLEDGMENT

The authors would like to thank the Associate Editor and anonymous reviewers for their valuable comments and suggestions, which greatly improved the quality of our paper.

REFERENCES

[1] X. Li, Z. Sun, D. Cao, H. Zhen, and Z. Qi, "Real-time trajectory planning for autonomous urban driving: Framework, algorithms, and verifications," *IEEE/ASME Transactions on Mechatronics*, vol. 21, no. 2, pp. 740 – 753, 2015.

[2] X. Li, Z. Sun, Z. He, Q. Zhu, and D. Liu, "A practical trajectory planning framework for autonomous ground vehicles driving in urban environments," in *Intelligent Vehicles Symposium (IV), 2015 IEEE*. IEEE, 2015, pp. 1160–1166.

[3] J. Leonard, J. How, S. Teller, M. Berger, S. Campbell, G. Fiore, L. Fletcher, E. Frazzoli, A. Huang, and S. Karaman, "A perception-driven autonomous urban vehicle," *Journal of Field Robotics*, vol. 25, no. 10, pp. 727–774, 2008.

[4] A. Bacha, C. Bauman, R. Faruque, M. Fleming, C. Terwelp, C. Reinholtz, D. Hong, A. Wicks, T. Alberi, and D. Anderson, "Odin: Team victortango's entry in the darpa urban challenge," *Journal of Field Robotics*, vol. 25, no. 8, pp. 467–492, 2008.

[5] B. J. Patz, Y. Papelis, R. Pillat, G. Stein, and D. Harper, "A practical approach to robotic design for the darpa urban challenge," *Journal of Field Robotics*, vol. 25, no. 8, pp. 528–566, 2008.

[6] K. Macek, R. Philippsen, and R. Siegwart, "Path following for autonomous vehicle navigation with inherent safety and dynamics margin," in *Intelligent Vehicles Symposium, 2008 IEEE*. IEEE, Conference Proceedings, pp. 108–113.

[7] J. Ziegler, P. Bender, M. Schreiber, H. Lategahn, T. Strauss, C. Stiller, T. Dang, U. Franke, N. Appenrodt, and C. Keller, "Making bertha drive? an autonomous journey on a historic route," *Intelligent Transportation Systems Magazine, IEEE*, vol. 6, no. 2, pp. 8–20, 2014.

[8] R. Attia, R. Orjuela, and M. Basset, "Combined longitudinal and lateral control for automated vehicle guidance," *Vehicle System Dynamics*, vol. 52, no. 2, pp. 261–279, 2014.

[9] P. Cartade, J.-B. Braconnier, R. Lenain, and B. Thuilot, "Adaptive and predictive control of a mobile robots fleet: Application to off-road formation regulation," in *IEEE International Conference on Robotics and Automation*. IEEE, 2013, Conference Proceedings, pp. 1836–1842.

[10] M. Werling, L. Gröll, and G. Bretthauer, "Invariant trajectory tracking with a full-size autonomous road vehicle," *IEEE Transactions on Robotics*, vol. 26, no. 4, pp. 758–765, 2010.

[11] J. M. Snider, "Automatic steering methods for autonomous automobile path tracking," Robotics Institute, Pittsburgh, PA,, Report Tech. Rep. CMU-RI-TR-09-08, 2009.

[12] S. Thrun, M. Montemerlo, H. Dahlkamp, D. Stavens, A. Aron, J. Diebel, P. Fong, J. Gale, M. Halpenny, and G. Hoffmann, "Stanley: The robot that won the darpa grand challenge," *Journal of field Robotics*, vol. 23, no. 9, pp. 661–692, 2006.

[13] G. M. Hoffmann, C. J. Tomlin, D. Montemerlo, and S. Thrun, "Autonomous automobile trajectory tracking for off-road driving: Controller design, experimental validation and racing," in *American Control Conference, 2007. ACC'07*. IEEE, Conference Proceedings, pp. 2296–2301.

[14] Z. Sun, Q. Chen, Y. Nie, D. Liu, and H. He, "Ribbon model based path tracking method for autonomous land vehicle," in *Intelligent Robots and Systems (IROS), 2012 IEEE/RSJ International Conference on*. IEEE, Conference Proceedings, pp. 1220–1226.

[15] D. Anderson, "Splined speed control using spam (speed-based acceleration maps) for an autonomous ground vehicle," Thesis, 2008.

[16] R. Rajamani, H.-S. Tan, B. K. Law, and W.-B. Zhang, "Demonstration of integrated longitudinal and lateral control for the operation of automated vehicles in platoons," *Control Systems Technology, IEEE Transactions on*, vol. 8, no. 4, pp. 695–708, 2000.

[17] S. E. Li, S. Xu, G. Li, and B. Cheng, "Periodicity based cruising control of passenger cars for optimized fuel consumption," in *Intelligent Vehicles Symposium Proceedings, 2014 IEEE*. IEEE, Conference Proceedings, pp. 1097–1102.

[18] J. Wang, Z. Sun, X. Xu, D. Liu, J. Song, and Y. Fang, "Adaptive speed tracking control for autonomous land vehicles in all-terrain navigation: An experimental study," *Journal of Field Robotics*, vol. 30, no. 1, pp. 102–128, 2013.

[19] J. Prez, V. Milans, and E. Onieva, "Cascade architecture for lateral control in autonomous vehicles," *Intelligent Transportation Systems, IEEE Transactions on*, vol. 12, no. 1, pp. 73–82, 2011.